Study of Flow Circulation inside Lid Driven Cavity for Low Reynolds Number

[1]Anitha L., [2]Venu Illandula, [3]Siddhartha Kosti

[1,2]*Assistant Professor, Sreechaitanya College of Engineering Timmapur, karimnagar*
[3]*Assistant Professor, Mechanical Engineering Department, SRCEM Banmore*

Abstract: *Present work here deal with finite difference simulation of the Navier-Stokes equation (mass and momentum) inside a lid driven cavity. Stream-vorticity approach has been adopted to solve the conservation equation of mass and momentum. Taylor's series has been used to convert the partial differential term into algebraic form. Central scheme has been adopted over forward and backward scheme because of the higher accuracy. Reynoldnumber governs the physical problem inside the cavity. Three different Reynold numbers 300, 400 and 500 have been considered. Grid validation test has been performed to validate the code. Contours of stream-function and vorticity has been represented and studied for different values of Reynold numbers. Results reveal that increment in Reynolds number increases the intensity of the extra circulation of streamlines and produces an extra roll in contours of horizontal and vertical velocities. From the results it has been found that peaks of the horizontal and vertical velocity increases with increment in the Reynolds number. Thinner vortices start to form near the lower lid with increment in the Reynolds number.*
Keywords: *Reynolds number, lid driven cavity, flow circulation*

I. Introduction

Lid driven cavity has been extensively studied by many researchers because of its many different applications. (N. A. C. Sidik and S. M. R. Attarzadeh, 2011) studied the cubic interpolated pseudo particle method and validate their results with the shear driven flow in shallow cavities. (Li et al., 2011) in their study applied the new version of multiple relaxation timesin lattices Boltzmann method to investigate the fluid flow in deep cavity.

(Manca et al., 2003) reported their study on laminar mixed convection for Reynolds numbers from 100 to 1000. They considered the aspect ratio in the ranges from 0.1 to 1.5. In their study they concluded that at higher Reynolds number maximum decrease in temperature occurred. The effect of the ratio of channel height to the cavity height was found to be played a significant role on streamlines and isotherm patterns for different heating configurations. The investigation also indicates that opposing forced flow configuration has the highest thermal performance, in terms of both maximum temperature and average Nusselt number.

(Khanafer et al. 2007) used pure-fluid and oscillating sinusoidal lid-driven and noticed that average Nusselt number increases with Grashof number and decreases with an increase in Reynolds number and lid frequency. (Gau and Sharif, 2004) reported mixed convection in rectangular cavities at various aspect ratios with moving isothermal side walls and constant flux heat source on the bottom wall.

Problem Statement:

Fig. 1 shows Schematic of square cavity. From fig. 1 one can notice that upperlid of cavity is moving with velocity u. While other boundaries have no-slip velocity boundary condition. As there is no direct equation available for pressure calculation for incompressible flow stream-vorticity approach has been used to solve governing equations.
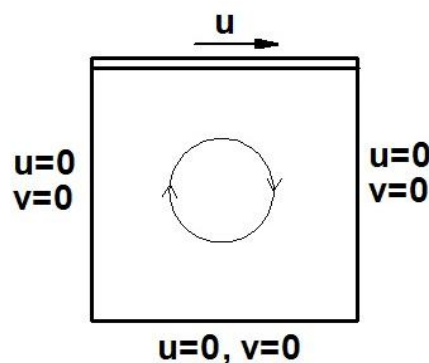

Fig. 1 Schematic of square cavity

Governing Equation
Velocity and Stream-function relationship

$$u = \frac{\partial \psi}{\partial y}, v = -\frac{\partial \psi}{\partial x}$$

Stream-function and Vorticity relationship

$$\omega = \frac{\partial v}{\partial x} - \frac{\partial u}{\partial y} = -\left(\frac{\partial^2 \psi}{\partial x^2} + \frac{\partial^2 \psi}{\partial y^2}\right)$$

Vorticity Transport Equation

$$\frac{\partial \omega}{\partial t} + u\frac{\partial \omega}{\partial x} + v\frac{\partial \omega}{\partial y} = \frac{1}{Re}\left(\frac{\partial^2 \omega}{\partial x^2} + \frac{\partial^2 \omega}{\partial y^2}\right)$$

Boundary Conditions
Initial Conditions

$$at\ t = 0 \rightarrow u = 0, v = 0, \psi = 0, \omega = 0$$

Wall Boundary Conditions
- *At the Left Vertical wall (x=0)*

$$x = 0 \rightarrow u = 0, v = 0, \psi = 0, \omega = -\frac{\partial^2 \psi}{\partial x^2}$$

- *At the Right Vertical wall (x=L)*

$$x = L \rightarrow u = 0, v = 0, \psi = 0, \omega = -\frac{\partial^2 \psi}{\partial x^2}$$

- *At the Bottom wall (y=0)*

$$y = 0 \rightarrow u = 0, v = 0, \psi = 0, \omega = -\frac{\partial^2 \psi}{\partial y^2}$$

- *At the Top Wall (y=L)*

$$y = 0 \rightarrow u = 0, v = 0, \psi = 0, \omega = -\frac{\partial^2 \psi}{\partial y^2}$$

Non-Dimensional Numbers

$$Re = \frac{\rho v D}{\mu}$$

Grid Generation
Physical domain has been discretized into small rectangular four nodded elements. A non-uniform collocated grid has been used for better accuracy at the walls of the enclosure. A collocated grid is what in which all the field variables (vectors as well as scalars) are defined at the same point of a cell. Figure shows the non-uniform collocated grid where element φ (i, j) represents the velocity component, stream-function, vorticity and temperature at the ith and j[th] node.
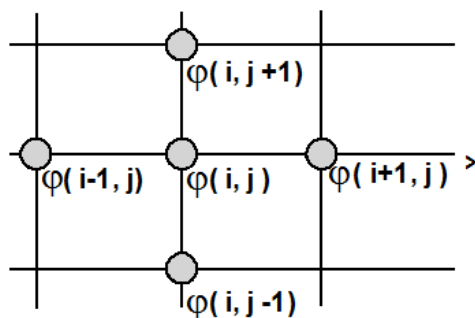

Fig.2: grid layout

II. Mathematical Modelling

Finite Difference Schemes
Main step in establishing a finite difference procedure to solve the partial differential equation is conversion of continuous problem into algebraic form by finite difference grid or mesh. As in the present problem we wish to find the flow distribution considering this in mind, ψ(x, y) in domain 0 ≤ x ≤ Land 0 ≤ y ≤ H we will develop a grid, replacing ψ(x, y) by ψ(iΔx, jΔy). From this we can locate the points by changing the values of i and j so that the equation can be written in terms of general nodes (i, j) and neighbours nodes. This has been represented in fig. 2. We can write as shown in table 1.

Table 1 Algebraic and vector notation of a point

Algebraic notation	Vector notation
x, y	i, j
x+Δx, y	i+1, j
x, y+Δy	i, j+1
x-Δx, y	i-1, j
x, y-Δy	i, j-1
x+Δx, y+Δy	i+1, j+1
x+2Δx, y	i+2, j
x, y+2Δy	i, j+2
x-2Δx, y	i-2, j
x, y-2Δy	i, j-2
x+2Δx, y+2Δy	i+2, j+2

Governing equations involved in the present problem are in partial differential form; to solve these equations first we have to convert these equations into algebraic form. For this Taylor series expansion has been utilizedfor X-direction and Y-direction.

By using Taylor series we can write the governing equation of the present problem in the form shown below.

$$u_{i,j} = \frac{\partial \psi}{\partial y} = \frac{\psi_{i,j+1} - \psi_{i,j-1}}{2\Delta y}$$

$$v_{i,j} = -\frac{\partial \psi}{\partial x} = -\frac{\psi_{i+1,j} - \psi_{i-1,j}}{2\Delta x}$$

$$\omega = -\left(\frac{\partial^2 \psi}{\partial x^2} + \frac{\partial^2 \psi}{\partial y^2}\right) = -\left(\frac{\psi_{i+1,j} + \psi_{i-1,j} - 2\psi_{i,j}}{\Delta x^2} + \frac{\psi_{i,j+1} + \psi_{i,j-1} - 2\psi_{i,j}}{\Delta y^2}\right)$$

Now to convert the vorticity transport equation which has the temporal derivative term can be discretized either by explicit scheme or by implicit scheme,

$$\frac{f_{i,j}^{n+1} - f_{i,j}^{n}}{\Delta t} = \nu\left(\frac{f_{i+1,j}^{n} + f_{i-1,j}^{n} - 2f_{i,j}^{n}}{(\Delta x)^2}\right), \frac{f_{i,j}^{n+1} - f_{i,j}^{n}}{\Delta t} = \nu\left(\frac{f_{i+1,j}^{n+1} + f_{i-1,j}^{n+1} - 2f_{i,j}^{n+1}}{(\Delta x)^2}\right)$$

Above equations represent the explicit and implicit discritization of equation. In explicit scheme only one term is unknown while all other terms are known, while in implicit scheme spatial derivative terms are also at the next time level (n+1) which makes it difficult to handle in computer code. It is easier to code the explicit scheme but requires a condition to satisfy, known as stability condition and leaves a limit on the time step for a particular grid selection while implicit scheme is free of this stability condition, represented in eq. below.

$$\nu \times \left(\frac{dt}{(dx)^2} + \frac{dt}{(dy)^2}\right) \leq \frac{1}{2}$$

In the present study explicit scheme has been considered for simplicity of the scheme, as we know that term at time 'n+1' is unknown while terms at time 'n' are known. So from above equation it can be observed that all the terms on right hand side are at time 'n' (known) while only one term at time 'n+1' is there in left hand side which can be easily calculated as,

$$\frac{\omega_{i,j}^{n+1} - \omega_{i,j}^{n}}{\Delta t} + u_{i,j}\frac{\omega_{i+1,j}^{n} - \omega_{i-1,j}^{n}}{2\Delta x} + v_{i,j}\frac{\omega_{i,j+1}^{n} - \omega_{i,j-1}^{n}}{2\Delta y}$$

$$= \frac{1}{Re}\left(\frac{\omega_{i+1,j}^{n} + \omega_{i-1,j}^{n} - 2\omega_{i,j}^{n}}{(\Delta x)^2} + \frac{\omega_{i,j+1}^{n} + \omega_{i,j-1}^{n} - 2\omega_{i,j}^{n}}{(\Delta y)^2}\right)$$

$$\omega_{i,j}^{n+1} = \omega_{i,j}^{n} + \Delta t\left(-u_{i,j}\frac{\omega_{i+1,j}^{n} - \omega_{i-1,j}^{n}}{2\Delta x} - v_{i,j}\frac{\omega_{i,j+1}^{n} - \omega_{i,j-1}^{n}}{2\Delta y}\right.$$

$$\left. + \frac{1}{Re}\left(\frac{\omega_{i+1,j}^{n} + \omega_{i-1,j}^{n} - 2\omega_{i,j}^{n}}{(\Delta x)^2} + \frac{\omega_{i,j+1}^{n} + \omega_{i,j-1}^{n} - 2\omega_{i,j}^{n}}{(\Delta y)^2}\right)\right)$$

Stability condition

$$\nu \times \left(\frac{dt}{(dx)^2} + \frac{dt}{(dy)^2}\right) \leq \frac{1}{2}$$

Above relation is the stability condition for two-dimensional problem. In case of violation of the above relation either code will diverge or results will be inaccurate.

III. Results and Discussion

Results have been presented here for different values of Reynolds number considered. Contours of stream-function, horizontal velocity, vertical velocity and vorticity have been presented to see the effect of the Reynolds number on the flow circulation and vortices generated inside the cavity. Line curve of horizontal velocity and vertical velocity have also been presented.

Figure 3 represents the contour of stream function inside the driven cavity for different values of Reynolds number considered. Contour of stream functions also known as streamlines are the quantity which physically represents the flow distribution. It can be noticed from the figures that with increment in the Reynolds number counter clockwise circulation starts to grow and for larger Reynolds their size is increasing continuously. For smaller Reynolds number clockwise streamlines are covering almost full part of the cavity but with increment in number its area is decreasing. It can also be noticed that for small Reynolds number a triangular shape counter clockwise streamline is forming on the right-bottom corner of the cavity and with increment in the Reynolds it is shifting towards the left side and also towards the center of the cavity.
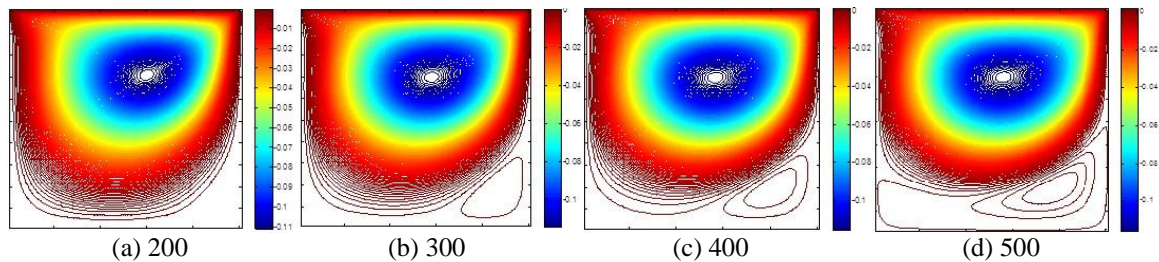

(a) 200	(b) 300	(c) 400	(d) 500

Figure 3: Contours of streamlines for different values of Re

Figure 4 and 5 represents the contours of horizontal velocity and vertical velocity. It can be noticed from the contours of velocities that two counter clockwise rolls are forming for both the velocities. It can be noticed from the figures that for horizontal velocity contours are forming near to the horizontal axis while for vertical velocity contours are forming near to the vertical axis. For horizontal velocity a small extra roll is forming near to the bottom-right corner of the cavity and with increment in the Reynolds its size and shape is changing continuously. Its shape is changing from parabolic to triangular shape from Reynolds number 200 to 500. For vertical velocity an extra roll on bottom-right corner start to form at Reynolds of 300 then another roll forms at bottom-left corner for Reynolds number of 500. Change in shape of first extra roll clockwise rolls with increment in the Reynolds number is noticeable.
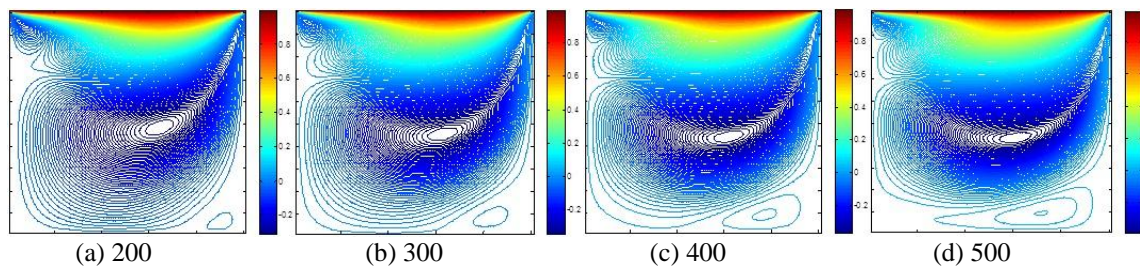

(a) 200	(b) 300	(c) 400	(d) 500

Figure 4: Contours of horizontal velocity for different values of Re

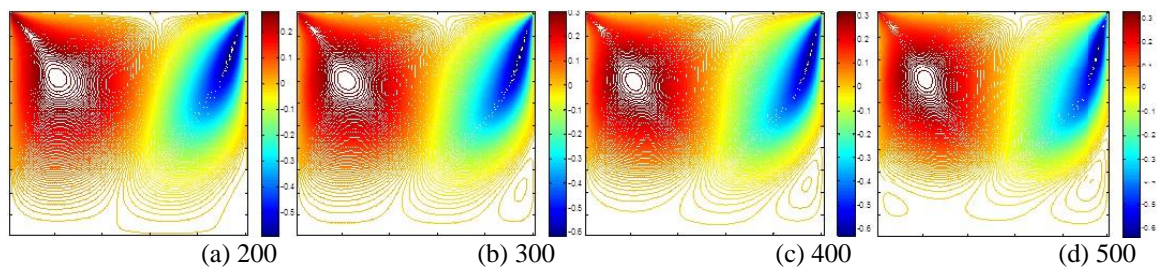|			
(a) 200	(b) 300	(c) 400	(d) 500

Figure 5: Contours of vertical velocity for different values of Re

Figure 6 represents the contour of the vorticity for different values of Reynolds number. Vortices are forming near to the upper side of the cavity which is due the fact that the upper lid is in motion or have a given velocity. And with increment in the Reynolds number more zigzag patterns starts to form near to the lower lid of the cavity.
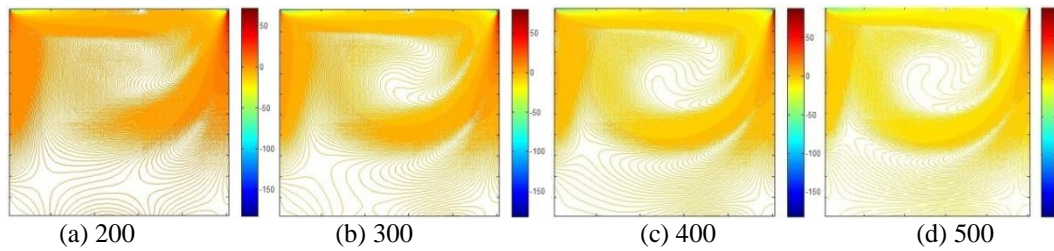
(a) 200   (b) 300   (c) 400   (d) 500

Figure 6: Contours of vorticity for different values of Re

Figure 7 and 8 represents the line curves of the horizontal and vertical velocity for different values of Reynolds number considered. Horizontal velocity has been plotted along the length and mid height of the cavity while vertical velocity has been plotted along the height and mid length of the cavity. Differences between the curves are easily noticeable. It can be observed that with increment in the Reynolds number velocities curves have large peak values compared to the low values of Reynolds number.
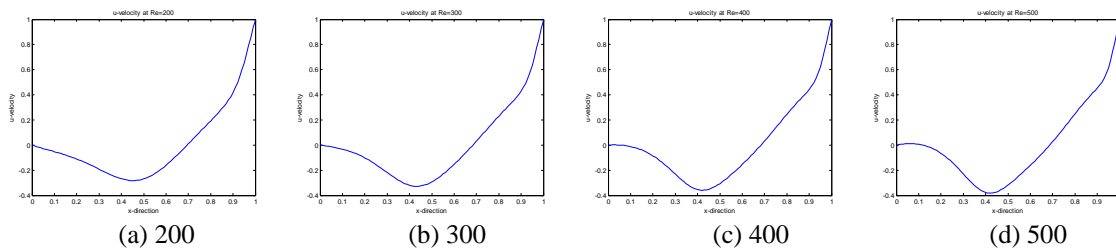

(a) 200   (b) 300   (c) 400   (d) 500

Figure 7: Horizontal velocity along length for different values of Re

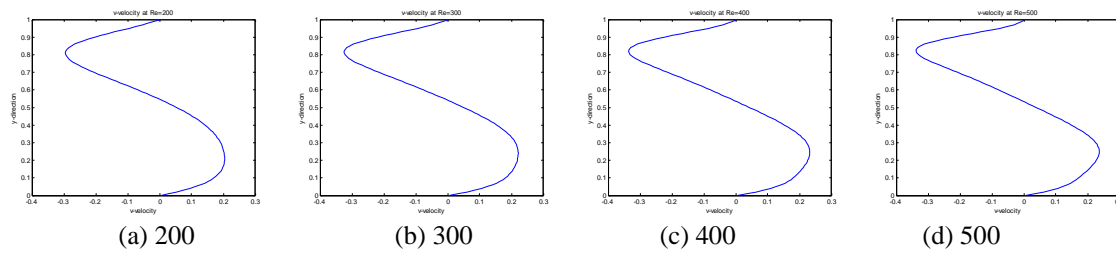(a) 200   (b) 300   (c) 400   (d) 500

Figure 8: Vertical velocity along length for different values of Re

IV. Conclusion

- Increment in Reynolds number increases the intensity of the extra circulation of streamlines.
- Increment in Reynolds number produces an extra roll in contours of horizontal and vertical velocities.
- Peaks of the horizontal and vertical velocity increases with increment in the Reynolds number.
- Thinner vortices start to form near the lower lid with increment in the Reynolds number.

References

[1]. Chen S,Large-eddy-based lattice Boltzmann model for turbulent flow simulation. Applied Mathematics and Computation, 2009, 591–595.
[2]. N. A. C. Sidik and S. M. R. Attarzadeh, An accurate numerical prediction of solid particle fluid flow in a lid-driven cavity. Intl. J. Mech. 2011, 5(3): 123-128.
[3]. S.L. Li, Y.C. Chen, and C.A. Lin. Multi relaxation time lattice Boltzmann simulations of deep lid driven cavity flows at different aspect ratios. Computer& Fluids, 2011, 45(1): 233-240.
[4]. A.J. Chamkha, Hydromagnetic combined convection flow in a vertical lid-driven cavity with internal heat generation or absorption, Numerical Heat Transfer, Part A, vol. 41, pp.529-546, 2002.
[5]. K.M. Khanafer, A.M. Al-Amiri and I. Pop, Numerical simulation of unsteady mixed convection in a driven cavity using an externally excited sliding lid, European Journal Mechanics B/Fluids, vol. 26, pp.669-687, 2007.
[6]. G.K. Batchelor. On Steady Laminar Flow with Closed Streamlines at Large Reynolds Numbers. Journal Fluid Mech. 1956; 1:177–190.
[7]. Kosti, S., Das, M.K. and Saha, A.K., Buoyancy-driven flow and heat transfer in a nanofluid-filled enclosure, Nanomaterials and Energy, 2013, 2(4), 200-211.
[8]. Kosti, S., Das, M.K. and Saha, A.K., Effect of nano-fluids on buoyancy-driven flow in a two-dimensional rectangular cavity, Proceedings of 22nd National and 11th International ISHMT-ASME Heat and Mass Transfer Conference December 28-31, IIT Kharagpur, India 2013.
[9]. Kosti, S., Natural convection in nanofluid-filled enclosure with heat flux boundary. Journal of Mechanical Engineering and Technology, 2014, 6(2), 1-12.
[10]. Kosti, S., Numerical study of heat flux boundary in a nano-fluid filled cavity, Nanomaterials and Energy, 2014, 2(4), 200-211.